



HAL
open science

Natural chalcones elicit formation of specialized pro-resolving mediators and related 15-lipoxygenase products in human macrophages

Christian Kretzer, Paul Jordan, Katharina P.L. Meyer, Daniel Hoff, Markus Werner, Robert Klaus Hofstetter, Andreas Koeberle, Antonio Cala Peralta, Guillaume Viault, Denis Seraphin, et al.

► To cite this version:

Christian Kretzer, Paul Jordan, Katharina P.L. Meyer, Daniel Hoff, Markus Werner, et al. Natural chalcones elicit formation of specialized pro-resolving mediators and related 15-lipoxygenase products in human macrophages. *Biochemical Pharmacology*, 2022, 195, pp.114825. 10.1016/j.bcp.2021.114825 . hal-03533844

HAL Id: hal-03533844

<https://univ-angers.hal.science/hal-03533844>

Submitted on 22 Sep 2023

HAL is a multi-disciplinary open access archive for the deposit and dissemination of scientific research documents, whether they are published or not. The documents may come from teaching and research institutions in France or abroad, or from public or private research centers.

L'archive ouverte pluridisciplinaire **HAL**, est destinée au dépôt et à la diffusion de documents scientifiques de niveau recherche, publiés ou non, émanant des établissements d'enseignement et de recherche français ou étrangers, des laboratoires publics ou privés.

Natural chalcones elicit formation of specialized pro-resolving mediators and related 15-lipoxygenase products in human macrophages

Christian Kretzer^a, Paul M. Jordan^a, Katharina P. L. Meyer^a, Daniel Hoff^a, Markus Werner^a, Robert Klaus Hofstetter^a, Andreas Koeberle^{a,b}, Antonio Cala Peralta^c, Guillaume Viault^c, Denis Seraphin^c, Pascal Richomme^c, Jean-Jacques Helesbeux^c, Hermann Stuppner^d, Veronika Temml^e, Daniela Schuster^e, Oliver Werz^{a,*}

* Corresponding author

^a Department of Pharmaceutical/Medicinal Chemistry, Institute of Pharmacy, Friedrich Schiller University Jena, Philosophenweg 14, 07743 Jena, Germany

^b Michael Popp Institute and Center for Molecular Biosciences Innsbruck (CMBI), University of Innsbruck, 6020 Innsbruck, Austria

^c Univ Angers, SONAS, SFR QUASAV, F-49000 Angers, France

^d Institute of Pharmacy/Pharmacognosy, Center for Molecular Biosciences Innsbruck (CMBI), University of Innsbruck, Innrain 80/82, 6020 Innsbruck, Austria

^e Department of Pharmaceutical and Medicinal Chemistry, Paracelsus Medical University Salzburg, 5020 Salzburg, Austria

Abstract

Specialized pro-resolving mediators (SPMs) comprise lipid mediators (LMs) produced from polyunsaturated fatty acids (PUFAs) via stereoselective oxygenation particularly involving 12/15-lipoxygenases (LOXs). In contrast to pro-inflammatory LMs such as leukotrienes formed by 5-LOX and prostaglandins formed by cyclooxygenases, the SPMs have anti-inflammatory and inflammation-resolving properties. Although glucocorticoids and non-steroidal anti-inflammatory drugs (NSAIDs) that block prostaglandin production are still prime therapeutics for inflammation-related diseases despite severe side-effects, novel concepts focus on SPMs as immunoresolvents for anti-inflammatory pharmacotherapy. Here, we studied the natural chalcone MF-14 and the corresponding dihydrochalcone MF-15, both isolated from *Melodorum fruticosum*, for modulating the biosynthesis of LM including leukotrienes, prostaglandins, SPM and their 12/15-LOX-derived precursors in human monocyte-derived macrophage (MDM) M1- and M2-like phenotypes. In MDM challenged with *Staphylococcus aureus*-derived exotoxins both compounds (10 μ M) significantly suppressed 5-LOX product formation but increased the biosynthesis of 12/15-LOX products, especially in M2-MDM. Intriguingly, in resting M2-MDM, both chalcones strikingly evoked generation of 12/15-LOX products and of SPMs from liberated PUFAs, along with translocation of 15-LOX-1 to membranous compartments. Enhanced 12/15-LOX product formation by the chalcones was evident also when exogenous PUFAs were supplied, excluding increased substrate supply as sole underlying mechanism. Rather, MF-14 and MF15 stimulate the activity of 15-LOX-1, supported by experiments with HEK293 cells transfected with either 5-LOX, 15-LOX-1 and 15-LOX-2. Together, the natural chalcones MF-14 and MF-15 favorably modulate LM biosynthesis in human macrophages by suppressing pro-inflammatory leukotrienes but stimulating formation of SPMs by differential interference with 5-LOX and 15-LOX-1.

Keywords: chalcones, 15-lipoxygenase, lipid mediators, specialized pro-resolving mediators, macrophages, inflammation resolution.

1. Introduction

Initiation, maintenance and resolution of acute inflammation are well-orchestrated processes regulated by lipid mediators (LMs) that are biosynthesized from free polyunsaturated fatty acids (PUFAs) [1]. Among these PUFAs, arachidonic acid (AA, ω -6) is metabolized at the onset of inflammation to prostaglandins and leukotrienes, generated by cyclooxygenases (COX) and by the 5-lipoxygenase (5-LOX) pathway, respectively, which promote the maintenance of inflammatory processes and contribute to related diseases like rheumatoid arthritis, atherosclerosis, respiratory disorders, Alzheimer's disease and cancer [2–4]. In contrast, resolution of inflammation is promoted by another superfamily of LMs that are specialized pro-resolving mediators (SPMs) encompassing resolvins (RVs), protectins (PDs) and maresins mainly produced by 12/15-LOXs from the ω -3 PUFAs eicosapentaenoic acid (EPA) or docosahexaenoic acid (DHA) [5]. These SPMs are highly potent signaling molecules blocking excessive neutrophil infiltration and pro-inflammatory cytokine secretion, increase the phagocytic and efferocytotic capacities of macrophages, and stimulate tissue repair and regeneration [6]. Common anti-inflammatory therapies such as the use of glucocorticoids and non-steroidal anti-inflammatory drugs (NSAIDs) suppress PG formation within this complex LM network, causing side effects due to substrate shunting into other non-targeted biosynthetic LM branches [7,8]. A novel concept pursues the support of inflammation resolution using application of SPMs and their precursors as well as elevation of endogenous SPM biosynthesis by supplementation of EPA and DHA [9]. Quite recently, manipulation of LM formation by natural products was reported that resulted in a shift from leukotrienes (LTs) and prostaglandins (PGs) to SPMs in the complex LM network by smart interference with 5-LOX at an allosteric site [10,11]. Here, we report on one chalcone and one dihydrochalcone that, apart from inhibiting 5-LOX and related LT formation, are able to stimulate

human monocyte-derived macrophages (MDM) for generation of SPM, apparently by cellular translocation and activation of 15-LOX-1.

Among natural products, flavonoids including chalcones have been in the focus of anti-inflammatory research for many years. Chalcones are ring-opened flavone-like structures and are widely distributed in daily consumables like vegetables, spices or various plants [12]. The structure of these types of compounds allows many different interactions with inflammation-related proteins [13]. In the analysis of new therapeutic options, natural and synthetic chalcones have been identified as anti-inflammatory agents that inhibit COX-2-derived PG formation and LT production involving 5-LOX [13–15]. In addition to the anti-inflammatory activities chalcones are also examined as antidepressant, analgesic and anticarcinogenic drugs [16,17]. Here, we investigated the natural chalcone MF-14 ((E)-1-[2,4-dihydroxy-3-[(2-hydroxyphenyl)methyl]-6-methoxy-phenyl]-3-(4-methoxyphenyl)prop-2-en-1-one) and the corresponding dihydrochalcone MF-15 (1-[2,4-dihydroxy-3-[(2-hydroxyphenyl)methyl]-6-methoxy-phenyl]-3-(4-methoxyphenyl)propan-1-one) (**Fig. 1A**), and are isolated from the leaves of *Melodorum fruticosum*. Previous studies showed that especially MF-15 facilitates strong antineoplastic effects as well as inhibition of androgen receptor signaling pathways and decreased aldo-keto reductase family 1 member C3 (AKR1C3) expression to treat enzalutamide resistant prostate cancer *in vitro* [18]. Our data demonstrate that in addition to their LT-suppressing actions via blocking 5-LOX, these chalcones act as elicitors of SPM biosynthesis in human macrophages implying potential as therapeutics for the treatment of inflammatory diseases.

Materials and methods

Isolation of MF-14 from *Melodorum fruticosum* was performed as previously described [18]. To obtain sufficient quantities for experimentation, MF-15 was semi-synthesized as described below from phlorizin that was efficiently extracted and purified from apple tree leaves. ^1H and ^{13}C NMR along with 2D NMR data were obtained on a JEOL JNM-ECZS 400 MHz spectrometer (400 and 100 MHz, respectively) in deuterated acetone and calibrated using the residual non-deuterated solvent resonance as internal reference. Chemical shifts (δ) are reported in ppm with (br) s used for (broad) singlet, d for doublet and t for triplet. Deuterium-labelled and non-labelled LM standards for ultra-performance liquid chromatography-tandem mass spectrometry (UPLC-MS-MS) quantification were obtained from Cayman Chemical/Biomol (Hamburg, Germany). All other chemicals were obtained at Sigma-Aldrich (Taufkirchen, Germany) unless stated otherwise.

2.1. Semi-synthesis of MF-15

(*E*)-1-[2,4-Bis(methoxymethoxy)-6-hydroxyphenyl]-3-(4-hydroxyphenyl)prop-2-en-1-one (di-MOM-phloretin, **compound 1**): To a solution of phloretin (92 mg, 0.34 mmol) in dry tetrahydrofuran (THF) (5 mL) MOM-Br (0.07 mL, 2.2 eq.) and diisopropylamine (0.15 mL, 2.5 eq.) were successively added at 0 °C. The reaction mixture was stirred at room temperature (RT) for 20 minutes. Then, it was diluted with 10 mL of water, neutralized with 1 M aqueous HCl and extracted with 3 × 15 mL of EtOAc. Combined organic layers were dried over Na_2SO_4 , filtered and evaporated under reduced pressure. The crude was purified by silica-gel column chromatography eluted with a mixture of petroleum ether/acetone (gradient from 9:1 to 7:3)

leading to 66 mg of di-MOM-phloretin **1** (54% yield). ¹H NMR (δ ppm, (CD₃)₂CO, 400 MHz): 13.72 (br s, 1H), 8.13 (br s, 1H), 7.10 (d, *J* = 8.4 Hz, 2H), 6.75 (d, *J* = 8.4 Hz, 2H), 6.30 (d, *J* = 2.3 Hz, 1H), 6.21 (d, *J* = 2.3 Hz, 1H), 5.35 (s, 2H), 5.24 (s, 2H), 3.48 (s, 3H), 3.44 (s, 3H), 3.37 (t, *J* = 7.7 Hz, 2H), 2.90 (t, *J* = 7.7 Hz, 2H). ¹³C NMR (δ ppm, (CD₃)₂CO, 100 MHz): 206.0, 167.7, 164.4, 161.3, 156.4, 133.1, 130.2, 116.0, 107.3, 97.6, 95.6, 95.0, 94.8, 57.0, 56.5, 46.9, 30.4.

(*E*)-1-[2,4-Bis(methoxymethoxy)-6-methoxyphenyl]-3-(4-methoxyphenyl)prop-2-en-1-one

(compound 2): NaH (195 mg, 3 eq.) and methyl iodide (0.71 mL, 5.9 eq.) were successively added to a solution of di-MOM-phloretin **1** (700 mg, 1.93 mmol) in 27 mL of dry THF at 0 °C. The resulting reaction mixture was stirred at the same temperature for 1.5 h. Then, 10 mL of ice-cold water were added and the mixture was extracted with 3 × 30 mL of EtOAc. Combined organic layers were dried over Na₂SO₄, filtered and evaporated under reduced pressure. The crude was purified by silica-gel column chromatography eluted with a mixture of petroleum ether/acetone (9:1) leading to 520 mg of **compound 2** (69% yield). ¹H NMR (δ ppm, (CD₃)₂CO, 400 MHz): 7.15 (d, *J* = 8.4 Hz, 2H), 6.83 (d, *J* = 8.4 Hz, 2H), 6.47 (d, *J* = 2.0 Hz, 1H), 6.40 (d, *J* = 2.0 Hz, 1H), 5.20 (s, 2H), 5.12 (s, 2H), 3.76 (s, 3H), 3.75 (s, 3H), 3.44 (s, 3H), 3.38 (s, 3H), 2.98 (t, *J* = 7.4 Hz, 2H), 2.88 (t, *J* = 7.4 Hz, 2H). ¹³C NMR (δ ppm, (CD₃)₂CO, 100 MHz): 202.3, 160.5, 158.9, 158.6, 156.0, 134.3, 130.1, 116.5, 114.5, 96.7, 95.4, 95.2, 94.7, 56.4, 56.3, 56.2, 55.4, 47.1, 29.4.

(*E*)-1-[2,4-Bis(hydroxy)-6-methoxyphenyl]-3-(4-methoxyphenyl)prop-2-en-1-one (**compound**

3): **Compound 2** (345 mg, 0.88 mmol) was dissolved in 16 mL of a 7:1 mixture EtOH/CH₂Cl₂. An excess of pTSA (2.05 g, 13.6 eq.) was added. The reaction mixture was stirred at 60 °C for 1 h. Then, approximately half of the solvents were evaporated under reduced pressure. The resulting

solution was diluted with water (20 mL) and saturated aqueous NaHCO₃ solution up to pH 6, extracted with 3 × 30 mL of EtOAc. Combined organic layers were dried over Na₂SO₄, filtered and evaporated under reduced pressure. The crude was purified by silica-gel column chromatography eluted with a mixture of petroleum ether/acetone (9:1) leading to 201 mg of 3 (75% yield). All spectroscopic data were in accordance with the ones reported for the corresponding natural derivative [19].

(*E*)-1-[2,4-Bis(hydroxy)-3-(2-hydroxybenzyl)-6-methoxyphenyl]-3-(4-methoxyphenyl)prop-2-en-1-one (MF-15): 2',4'-dihydroxy-4,6'-dimethoxydihydrochalcone 3 (83.6 mg, 0.277 mmol), 2 mL dry dioxane, 2-hydroxybenzyl alcohol (34.4 mg, 1 eq.) and ZnCl₂ (35 mg, 1 eq.) were transferred into a microwave reactor. Then, the reaction mixture was irradiated at 130 °C for 0.5 h. It was quenched by adding 10 mL H₂O, extracted with 3 × 10 mL EtOAc. Combined organic layers were dried over Na₂SO₄, filtered and evaporated under reduced pressure. The crude was purified by silica-gel column chromatography eluted with a mixture of petroleum ether/acetone (from 3:1 to 3:2 ratio) leading to 68 mg of MF-15 as a colorless solid (60% yield). All spectroscopic data were in accordance with the ones reported for the corresponding natural derivative [20].

2.2. Cell isolation and cell culture

Leukocyte concentrates were prepared from peripheral blood obtained from healthy human adult donors that received no anti-inflammatory treatment for the last 10 days (Institute of Transfusion Medicine, University Hospital Jena). The approval for the protocol was given by the ethical committee of the University Hospital Jena and all methods were performed in accordance with the

relevant guidelines and regulations. To isolate polymorphonuclear leukocytes (PMNL) and monocytes, the leukocyte concentrates were mixed with dextran (dextran from *Leuconostoc* spp. MW ~40,000) for sedimentation of erythrocytes; the supernatant was centrifuged on lymphocyte separation medium (Histopaque®-1077). Contaminating erythrocytes in the pelleted neutrophils were removed by hypotonic lysis using water. PMNL were then washed twice in ice-cold phosphate buffer saline (PBS) and finally resuspended in PBS. The peripheral blood mononuclear cell (PBMC) fraction on top of lymphocyte separation medium was washed with ice-cold PBS and seeded in cell culture flasks (Greiner Bio-one, Nuertingen, Germany) for 1.5 h (37 °C, 5% CO₂) in PBS with Ca²⁺/Mg²⁺ to isolate monocytes by adherence. For differentiation and polarization of monocytes to M1- and M2-like macrophages, we followed published procedures [21]. Thus, adherent monocytes were treated with 20 ng mL⁻¹ granulocyte macrophage-colony stimulating factor (GM-CSF) (Peprotech, Hamburg, Germany) for 6 days in RPMI 1640 supplemented with 10% fetal calf serum (FCS), 2 mmol L⁻¹ L-glutamine, penicillin (100 U mL⁻¹) and streptomycin (100 µg mL⁻¹) for differentiation and further incubated with 100 ng mL⁻¹ lipopolysaccharide (LPS) and 20 ng mL⁻¹ interferon-γ (Peprotech) for 48 h to get M1-MDM. To obtain M2-MDM, monocytes were treated with 20 ng mL⁻¹ M-CSF (Peprotech) for 6 days, followed by 20 ng mL⁻¹ interleukin (IL)-4 (Peprotech) for 48 h. Unpolarized M0-MDM were obtained by differentiation with M-CSF and GM-CSF (10 ng mL⁻¹, each) for 6 days. Correct polarization and purity of MDM was routinely checked by flow cytometry (LSRFortessa™ cell analyzer, BD Biosciences, Heidelberg, Germany) as reported [8] using the following antibodies: FITC anti-human CD14 (clone M5E2, BD Biosciences), APC-H7 anti-human CD80 (clone L307.4, BD Biosciences), PE-Cy7 anti-human CD54 (clone HA58, Biolegend, Koblenz, Germany), PE anti-human CD163 (clone GHI/61, BD Biosciences), and APC anti-human CD206 (clone 19.2, BD Bioscience). HEK293 cells were cultured in monolayers (37 °C, 5% CO₂) in DMEM containing FCS (10%), penicillin (100 U mL⁻¹) and streptomycin (100 µg mL⁻¹). HEK293 cell lines stably expressing 5-

LOX, 15-LOX-1 and 15-LOX-2 were selected using geneticin (400 μg) as reported [10]. Transfection of HEK293 cells was performed by using pcDNA3.1 plasmids and lipofectamine according to the manufacturer's protocol (Invitrogen, Darmstadt, Germany) and as reported before [22].

2.3. Expression, purification and activity assay of human recombinant 5-LOX

E.coli BL21 was transformed with pT3-5-LO plasmid at 30 °C overnight to express recombinant 5-LOX as described before [23]. The bacteria were treated with lysis buffer containing triethanolamine (50 mM, pH 8.0), EDTA (5 mM), phenylmethanesulfonyl fluoride (1 mM), soybean trypsin inhibitor (60 $\mu\text{g mL}^{-1}$), dithiothreitol (2 mM) and lysozyme (1 mg mL^{-1}) before sonification (3 \times 15 s) to obtain cell lysates. 5-LOX was purified from supernatants after centrifugation of the lysates (40,000 \times g; 20 min, 4 °C) by using an ATP-agarose column and diluted with PBS buffer containing 1 mM EDTA. For evaluation of 5-LOX product formation, 0.5 μg purified 5-LOX was diluted in 1 mL PBS containing 1 mM EDTA and pre-incubated with vehicle (0.1% DMSO) or test compounds for 15 min on ice and then stimulated with 20 μM AA and 2 mM CaCl_2 for 10 min at 37 °C. The reaction was stopped by addition of 1 mL ice-cold methanol containing PGB_1 (200 ng) as internal standard, and 5-LOX products (i.e., trans-isomers of LTB_4 and 5-H(P)ETE) were analyzed by RP-HPLC as described previously [24]. Briefly, 530 μl acidified PBS and 200 ng of internal PGB_1 standard were added and solid phase extraction (SPE) using C18 RP-columns (100 mg, UCT, Bristol, PA, USA) was performed. After elution with methanol, samples were analyzed by RP-HPLC using a C-18 Radial-PAK column (Waters, Eschborn, Germany).

2.4. Cytotoxicity assays in human MDM

Cytotoxicity was studied by analysis of lactate dehydrogenase (LDH) release (cell integrity) and by 3-(4,5-dimethyl-2-thiazolyl)-2,5-diphenyl-2H-tetrazolium bromide (MTT) assay (cell viability) in M0-MDM. The release of LDH from the cells was analyzed using the CytoTox 96® Non-Radioactive Cytotoxicity Assay (Promega GmbH, Mannheim, Germany). In brief, 10^6 M0-MDM per well were suspended in RPMI-medium containing 10% FCS, penicillin/streptomycin and L-glutamine, were seeded in a 24-well plate. Lysis control and 0.2% triton X-100 were added to the cells and incubated for 45 min; compounds and control (0.1% DMSO) were added and incubated for another 24 h at 37 °C. Stop solution was added, the plate was centrifuged ($250 \times g$, 4 min, RT) and 50 μ L of supernatant from each well was transferred in a 96-well plate. Afterwards, 50 μ L of substrate mixture was added and incubated for 30 min at RT in the dark. To finally stop the reaction, 50 μ L of stop solution were added. The photometric measurement was performed at 490 nm using a Multiskan Spectrum plate reader (Thermo Fischer) as reported before [25].

For analysis of cytotoxic effects by MTT assay [26], 10^5 M0-MDM per well were seeded in a 96 well plate (triplicates). Briefly, test compounds or controls (DMSO as vehicle control; staurosporine (1 μ M) as positive control) were added and incubated for 48 h (37 °C, 5% CO₂). Next, the MTT solution was added and cells were incubated for another 2 h under the aforementioned conditions. Then, 100 μ L SDS lysis buffer was added under gently shaking for 20 h at 175 rpm in the dark. VIS detection was used to measure the corresponding reaction at 570 nm.

2.5. Evaluation of 5-LOX product formation in human PMNL

For evaluation of 5-LOX product formation in human PMNL, 10^7 cells per mL PBS plus 1 mM CaCl_2 and 0.1% glucose were incubated with test compounds for 15 min at 37 °C and then stimulated with 2.5 μM Ca^{2+} -ionophore A23187 (Cayman, Ann Arbor, USA) for 10 min. The incubation was stopped with 1 mL ice-cold methanol containing 200 ng mL^{-1} PGB1 as internal standard. Samples were subjected to SPE and formed LM were separated and analyzed by RP-HPLC as described [27].

2.6. Determination of the lipid mediator profile in human MDM and in HEK293 cells

Human MDM (2×10^6 cells in 1 mL PBS plus 1 mM CaCl_2) were seeded in 6-well-plates and preincubated for 15 min with test compounds at 37 °C. The macrophages were subsequently incubated with 1% (v/v) *Staphylococcus (S.) aureus* 6850-conditioned medium (SACM, 24 h culture from OD = 0.05) for 3 h to induce LM formation, as reported recently [28]. Alternatively, MDM (2×10^6 cells in 1 mL PBS plus 1 mM CaCl_2) were incubated with the test compounds with or without AA, EPA, DHA (1 μM each) at 37 °C for 3 h min.

HEK293 cells (2×10^6 cells in 1 mL PBS plus 1 mM CaCl_2 and 0.1% glucose) were preincubated with test compounds or vehicle (0.1% DMSO) for 10 min at 37 °C, and LM biosynthesis was initiated by addition of 2.5 μM A23187 plus 1 μM AA for another 15 min at 37 °C. Alternatively, HEK293 cells were incubated with test compounds or vehicle (0.1% DMSO) together with AA, EPA, DHA (1 μM each) for 3 h at 37 °C.

Incubation of either MDM or HEK293 cells was stopped with 2 mL ice-cold methanol containing deuterium-labeled internal standards (d8-5S-HETE, d4-LTB₄, d5-LXA₄, d5-RvD2, and d4-PGE₂; 500 pg each). Samples were kept at -20 °C for one day to allow protein precipitation. After centrifugation (2000 × g, 4 °C, 10 min), 8 mL acidified water was added (final pH = 3.5) and samples were subjected to solid phase extraction using RP-18 columns. LMs were analyzed by UPLC-MS/MS [21].

2.7. SDS-PAGE and Western blot

Cell lysates of MDM (2×10^6 cells) were separated on 10% polyacrylamide gels and blotted onto nitrocellulose membranes (Amersham Protran Supported 0.45 μm nitrocellulose; GE Healthcare, Chicago, IL, USA). The membranes were incubated with the following primary antibodies: rabbit polyclonal anti-5-LOX, 1:1000 (Genscript, Piscataway, NJ, USA, to a peptide with the C-terminal 12 aa of 5-LOX: CSPDRIPNSVAI; kindly provided by Dr. Marcia Newcomer, Louisiana State University, Baton Rouge, LA, USA); mouse monoclonal anti-15-LOX-1, 1:500 (ab119774; Abcam, Cambridge, United Kingdom); rabbit polyclonal anti-COX-2, 1:500 (4842; Cell Signaling Technology); rabbit polyclonal anti-15-LOX-2, 1:500 (ab23691; Abcam), and rabbit polyclonal anti-β-actin, 1:1000 (4967S; Cell Signaling Technology). Immunoreactive bands were stained with IRDye 800CW goat anti-mouse IgG (H+L), 1:10,000 (926-32210; Li-Cor Biosciences, Lincoln, NE, USA), IRDye 800CW goat anti-rabbit IgG (H+L), 1:15,000 (926 32211; Li-Cor Biosciences) and IRDye 680LT goat anti-mouse IgG (H+L), 1:40,000 (926-68020; Li-Cor Biosciences), and visualized by an Odyssey infrared imager (Li-Cor Biosciences). Data from densitometric analysis were background corrected.

2.8. Flow cytometry

Cells were stained in PBS pH 7.4 containing 0.5% BSA, 2 mM EDTA and 0.1% sodium azide by Zombie Aqua™ Fixable Viability Kit (Biolegend, San Diego, CA, USA) for 5 min at 4 °C to determine cell viability. Non-specific antibody binding was blocked by using mouse serum (10 min at 4 °C) prior to staining by the following fluorochrome-labelled antibodies (20 min, 4 °C): FITC anti-human CD14 (clone M5E2, BD Biosciences), APC-H7 anti-human CD80 (clone L307.4, BD Biosciences), PE-Cy7 anti-human CD54 (clone HA58, Biolegend), PE anti-human CD163 (clone GHI/61, BD Biosciences), and APC anti-human CD206 to determine M1 and M2 surface marker expression using a LSRFortessa™ cell analyzer (BD Biosciences), and data were analyzed using FlowJo X Software (BD Biosciences).

2.9. Immunofluorescence microscopy

MDM (10^6 cells) were seeded onto glass coverslips in a 12-well plate and cultured for 48 h. SACM, test compounds or DMSO (0.1% as vehicle) were added at 37 °C and stopped after the indicated times by fixation with 4% paraformaldehyde solution. Acetone (3 min, 4 °C) followed by 0.25% Triton X-100 for 10 min at RT was used for permeabilization prior to blocking with normal goat serum 10% (50062Z, ThermoFisher). Coverslips were incubated with mouse monoclonal anti-15-LOX-1 antibody, 1:100 (ab119774, Abcam, Cambridge, UK) and rabbit anti-5-LOX antibody, 1:100 (1550 AK6, kindly provided by Dr. Olof Radmark, Karolinska Institutet, Stockholm,

Sweden) at 4 °C overnight. 5-LOX and 15-LOX-1 were stained with the fluorophore-labeled secondary antibodies; Alexa Fluor 555 goat anti-mouse IgG (H + L); 1:500 (A21424, ThermoFisher) and Alexa Fluor 488 goat anti-rabbit IgG (H + L), 1:500 (A11034, ThermoFisher). Samples were analyzed by a Zeiss Axiovert 200M microscope, and a Plan Neofluar ×40/1.30 Oil (DIC III) objective (Carl Zeiss, Jena, Germany). An AxioCam MR camera (Carl Zeiss) was used for image acquisition.

2.10. Statistical analysis

The sample size for experiments with MDM and PMNL was chosen empirically based on previous studies [21] to ensure adequate statistical power. The results are expressed as mean ± standard error of the mean (SEM) of n observations, where n represents the number of experiments with cells from separate donors, performed on different days, as indicated. Datasets were analyzed by GraphPad Prism 9.1.2 (GraphPad, La Jolla, CA, USA) using one-way ANOVA and ratio-paired t-test to overcome interindividual differences of human donors.

3. Results

3.1. The chalcones MF-14 and MF-15 inhibit 5-LOX product formation

Our previous in silico target prediction approach identified human 5-LOX as potential target of a variety of natural chalcones [15]. Here, we assessed the efficiency of the natural chalcone MF-14 and its corresponding dihydrochalcone MF-15 (**Fig. 1A**) to interfere with the activity of human 5-LOX in cell-free and cell-based assays. While MF-14 was isolated from *Melodorum fruticosum* as previously described [18], to obtain MF-15 in sufficient quantities, a semi-synthetic approach was used. Thus, hydrolysis of phlorizin yielded its aglycone, phloretin (Pt), as previously described [29]. Pt was then protected in positions 2' and 4' using MOMBr as alkylating agent in the presence of a base with an optimized yield of 54% for **compound 1** (**Fig. 1B**). The two remaining phenol functions of **1** were alkylated with methyl iodide leading to **2** (69%). Removal of the acetal protecting groups yielded **3**, already known as a secondary metabolite isolated from the trunk wood of *Iranthera laevis* Markgr [19]. Monobenylation of **3** using modified conditions from Urgaonkar et al. [30] allowed the synthesis of MF-15 with 60% yield for this step and an overall yield of 14% (5 steps) from phlorizin.

We studied inhibition of the enzymatic activity of isolated human 5-LOX and 5-LOX product formation in Ca^{2+} -ionophore A23187-activated human neutrophils, which both are well-established and convenient test systems for initial and routine studies of 5-LOX inhibitors, where respective mediators are analyzed by RP-HPLC (UV detection at 235 and 280 nm) [27]. The chalcone MF-14 with an $\text{IC}_{50} = 2.4 \pm 0.3 \mu\text{M}$ was more potent against isolated 5-LOX (**Fig. 1C**) than in neutrophils ($\text{IC}_{50} = 7.7 \pm 1 \mu\text{M}$; **Fig. 1D**), while the corresponding dihydrochalcone MF-15 showed similar potency in both experimental settings ($\text{IC}_{50} = 3.5 \pm 0.2 \mu\text{M}$ for isolated 5-LOX; $\text{IC}_{50} = 3.1 \pm 0.3 \mu\text{M}$ in neutrophils; **Fig. 1C, D**), thus, being somewhat superior over MF-14 in intact cells.

3.2. Modulation of LM profiles by MF-14 and MF-15 in exotoxin-stimulated human MDM

For more comprehensive analysis of the effects of the chalcones on broad and complex LM networks under pathophysiological relevant conditions, we used polarized human MDM with either pro-inflammatory (M1-) or anti-inflammatory (M2-like) phenotype that were stimulated by bacterial exotoxins for 3 h [8,21,28]. M1-MDM express abundant 5-LOX and FLAP but hardly 15-LOX-1, whereas M2-MDM express both 5-LOX/FLAP and substantial amounts of 15-LOX-1 [REF 21]. First, we investigated whether the chalcones are cytotoxic, displaying detrimental effects on the viability and integrity of MDM, using MTT assay and LDH release analysis. Neither MF-14 nor MF-15 up to 10 μ M significantly affected cellular viability of MDM in these assays over 24 h (**Fig. 2A,B**). At higher concentrations, i.e., 30 μ M, both compounds caused detrimental effects in both viability assays, prompting us to limit the concentrations for further investigations to \leq 10 μ M.

As reported before, upon exposure to bacterial exotoxins, M1-MDM produce mainly pro-inflammatory COX-derived PGs/TX and 5-LOX-derived LTs, while M2-MDM generate substantial amounts of SPM and their 15-LOX-1-derived monohydroxylated precursors [8,21,28]. We studied the LM profiles of M1- and M2-MDM by targeted LM metabololipidomics using UPLC-MS/MS [8]. M1-MDM produced higher amounts of various COX-derived LM (PGD₂ α , PGE₂, PGF₂ α and TXB₂) as compared to M2-MDM, without strong differences related to 5-LOX product (5-HEPE, 5-HETE, t-LTB₄, LTB₄ and 5S,6R-di-HETE) formation between the two phenotypes (**Table 1**). In contrast, formation of SPM (PD1, PDX, RvD5 and MaR1) and of other 12/15-LOX products (17-HDHA, 14-HDHA, 15-HEPE, 15-HETE, 12-HEPE, 12-HETE) was

much higher in M2-MDM. Preincubation of the MDM with MF-14 and MF-15 at 10 μ M, each, clearly inhibited the biosynthesis of SACM-induced 5-LOX products in both phenotypes (**Table 1**), where MF-15 appeared to be somewhat more efficient than MF-14, especially for inhibition of LTB₄. Among COX products, TXB₂ formation was reduced by MF-14 but less pronounced by MF-15 in both MDM subtypes, while PGs were hardly affected or rather elevated, in particular in M2-MDM (**Table 1**). Of interest, both chalcones enhanced the formation of 12/15-LOX products including SPMs, more consistently in M2- versus M1-MDM. Note that among these mono/di-hydroxylated PUFAs, MF-14 and MF-15 failed to elevate 4-HDHA, 7-HDHA and 5,15-diHETE that are not or not exclusively formed by 12/15-LOXs; the amounts of liberated PUFAs were all moderately increased by MF-14 and MF-15 in both MDM phenotypes (**Table 1**).

Next, the potency of MF-14 and MF-15 was studied in more detail in concentrations-response experiments (0.1 to 10 μ M) using SACM-activated MDM. In M1-MDM, formation of COX products and SPM as well as PUFA release were hardly affected by either chalcone, but again mono/di-hydroxylated 12/15-LOX metabolites were significantly increased, more pronounced by MF-15 versus MF-14, starting at 3 μ M MF-15 (**Fig. 2C**). 5-LOX products were suppressed only by MF-15 at 10 μ M. A comparable pattern of LM modulation was found in M2-MDM, where mono/di-hydroxylated 12/15-LOX products and SPM were most strikingly elevated with significant effects at 3 and 10 μ M for both chalcones, with some superiority for MF-15 (**Fig. 2D**). To estimate if the stimulatory effects of chalcones on LOX product formation depends on the type of substrate, we differentially analyzed the modulation of mono/di-hydroxylated products derived from either ω -6-PUFA (AA) or ω -3-PUFA (EPA and DHA). Obviously, those LOX products that require a C15- or C17-lipoxygenation such as 15-HETE and 15-HEPE or 17-HDHA, made from AA and EPA or DHA, respectively, were most prominently affected (**Fig. 2C, D**). This suggests

that the chalcones preferably stimulate C15-lipoxygenation in MDM irrespective of the type of PUFA substrate.

3.3. MF-14 and MF-15 preferably stimulate 15-LOX-1 activity in HEK cells

In humans, two isoforms 15-LOX-1 and 15-LOX-2 exist that not only differ in the cell type-dependent expression but also in the regiospecificity of PUFA oxygenation: while 15-LOX-2 (equally present at low amounts in human M1- and M2-MDM [28]; **Fig. 5B**) selectively catalyzes oxygenation of C15 in AA and EPA and C17 in DHA, 15-LOX-1 (abundant in human M2-MDM) also oxygenates C12 in AA and EPA and C14 in DHA, although to a minor degree versus C15 and C17 [31]. To further dissect if and which 15-LOX isoform confers the stimulatory effects of the chalcones, we took advantage of HEK293 cells stably transfected with either human 15-LOX-1 or 15-LOX-2; cells expressing human 5-LOX were studied as additional control. Preincubation of HEK293 cells with chalcones and subsequent stimulation with 2.5 μ M ionophore A23187 plus 1 μ M AA, according to previous studies [10,22], showed that both chalcones (10 μ M), again preferably MF-15, strongly elevated product formation (15-HETE, 15-HEPE, 17-HDHA and 14-HDHA) in cells expressing 15-LOX-1 but not so in cells expressing the 15-LOX-2 isoform (**Table 2, Fig. 2E**). In HEK293 cells expressing 5-LOX, strong suppression of 5-LOX products was obvious by MF-14 and MF-15 without significant elevation of 12/15-LOX products (**Table 2, Fig. 2E**), as expected. Conclusively, MF-14 and MF-15 inhibit 5-LOX product formation in PMNL and MDM but increase 12/15-LOX products and SPM formation in MDM.

3.4. MF-14 and MF-15 elicit formation of 12/15-LOX products and SPMs by stimulating 15-LOX-1

To gain further insights in whether MF-14 and MF-15 could induce 15-LOX-1 activation and thus elicit SPM formation in MDM without the need of an additional stimulus (such as SACM or ionophore), we simply exposed M1- and M2-MDM to the chalcones for 3 h and analyzed the LM formed by UPLC-MS/MS. In both MDM phenotypes, the chalcones induced LOX product formation versus vehicle control with similar effectiveness for MF14 and MF-15 and without affecting COX products (**Table 3, Fig. 3A, B**). Along these lines, the chalcones strongly elevated the liberation of PUFAs, a general prerequisite for enabling LM biosynthesis in intact cells. The stimulatory effects of the chalcones were most prominent for 12/15-LOX products in M2-MDM, especially for 15-HETE and 12-HETE with up to 68- and 74-fold increases, respectively, and also SPM were elevated up to 19-fold (**Table 3, Fig. 3A, B**). Note that also 5-LOX products were elevated by the chalcones but to a lower degree (max. up to 6-fold). The magnitude of 12/15-LOX product formation induced by the chalcones in M2-MDM is approx. 30-44% of that obtained with SACM, while 5-LOX products are only 2-5% (compare absolute quantities shown in Table 3 with those in Table 1). Concentration-response studies showed that in M2-MDM significant induction of 12/15-LOX products was achieved also at 3 μ M of either MF-14 or MF-15, whereas 5-LOX product formation was unaffected at this concentration (**Fig. 3A, B**). As observed for SACM-stimulated MDM, the chalcones consistently stimulated lipoxygenation irrespective of the type of substrate (ω 3- or ω 6-PUFA).

Activation of 15-LOX-1 and of 5-LOX and respective product formation in stimulated M2 macrophages is associated with subcellular redistribution of the enzymes from a soluble to a membranous compartment, where enzymatic transformation of the liberated PUFAs takes place [21,28]. Therefore, we studied the subcellular localization of 15-LOX-1, and for comparison of 5-LOX, in M2-MDM and how this is affected by the chalcones in a temporal manner (15, 30, 180 min) using immunofluorescence microscopy; SACM was used as a positive control [28]. In resting vehicle-treated cells, 5-LOX and 15-LOX-1 were diffusely distributed within the nucleus and cytosol, respectively, while addition of SACM caused 5-LOX enrichment at the nuclear envelope and 15-LOX-1 accumulation at yet undefined particulate structures after 30 min, as observed before [21,28]. The same 5-LOX and 15-LOX-1 subcellular redistribution pattern as for SACM was evident also for MF-14 and MF-15 (10 μ M) with even more rapid induction by MF-15 starting already at 15 min (**Fig. 3C**).

To exclude that simply the elevation of PUFA liberation accounts for elevated LOX product formation, we supplemented M2-MDM with substantial amounts of exogenous DHA, EPA and AA (1 μ M, each) to circumvent the requirement of endogenous substrate supply. As shown in **Table 4**, formation of 12/15-LOX products including SPM in response to MF-14 and MF-15 was still markedly elevated, up to 56-fold for 15-HETE, with a similar pattern for the overall LM profile as in the absence of exogenous substrate (**Table 3**). Finally, we studied if human LOXs in transfected HEK293 cells could be activated by the chalcones without additional stimulus but in the presence of DHA, EPA and AA (1 μ M, each). Again, MF-14 and even more efficiently MF-15 enhanced the formation of typical 12/15-LOX products in HEK293 cells expressing 15-LOX-1 but hardly in cells expressing the 15-LOX-2 isoform and less efficiently also in 5-LOX-transfected cells (**Fig. 4**). Together, MF-14 and MF-15 are able to substantially elicit 12/15-LOX

products including SPM in intact cells by two mechanisms: (i) induction of endogenous PUFA substrate release and (ii) selective and strong stimulation of the 15-LOX-1 isoform.

3.5. MF-14 and MF-15 do not affect MDM polarization and LM-biosynthetic enzyme expression

In addition to these short-term effects of the chalcones observed within approx. 3 h, we explored if MF-14 and MF-15 could also affect the polarization of MDM towards the M1 and M2 phenotype as well as expression of LM-biosynthetic key enzymes during 48 h of MDM polarization where the cells acquire these proteins in a phenotype-specific manner, i.e., COX-2 for M1- and 15-LOX-1 for M2-MDM. Flow cytometry analysis of CD54 and CD80 (markers for M1) as well as CD163 and CD206 (markers for M2) revealed no significant changes upon treatment of unpolarized MDM for 48 h in the presence of 10 μ M MF-15, but interestingly, treatment with 10 μ M MF-14 strongly reduced the expression of the M2 marker CD206, without any effects on CD54, CD80 or CD163 (**Fig. 5A**). Western blot analysis of COX-2, 5-LOX and 15-LOX-1 protein levels showed no significant modulation of their expression by the chalcones at 10 μ M during polarization to M1- or M2-MDM (**Fig. 5B**). These data indicate the chalcones MF-14 and MF-15 affect LM networks in polarized macrophages at the level of enzymatic biosynthesis of the LM but not primarily by modulation of MDM polarization or of LM-biosynthetic enzyme expression.

4. Discussion

Here we showed that the natural chalcone MF-14 and its corresponding dihydrochalcone MF-15, both isolated from *Melodorum fruticosum* leaves [18], suppress pro-inflammatory LT formation by inhibiting 5-LOX but elevate the generation of inflammation-resolving SPMs by stimulating cellular 15-LOX-1. Of note these SPM/15-LOX-1-stimulatory effects were evident not only in exotoxin-activated MDM but also when resting MDM, especially M2-MDM, were exposed to the chalcones. Both chalcones caused liberation of free PUFAs as LM substrates and induced 15-LOX-1 subcellular redistribution in M2-MDM, which are major prerequisites for LM formation in intact cells [21,28,31]. Inhibition of 5-LOX and stimulation of 15-LOX-1 in intact cells, with minor effects on the 15-LOX-2 isoform, was confirmed in activated as well as in resting HEK293 cells transfected with the respective LOX. Together, these chalcones are effective inhibitors of 5-LOX but also act as agonists for macrophages and non-immunocompetent (HEK293) cells to stimulate 15-LOX-1 activity which culminates in elevated SPM levels. Small molecules with such LM-modulatory ability, shifting the biosynthesis from pro-inflammatory to pro-resolving LM, are of great interest for innovative inflammation pharmacotherapy [6,9,32].

The major drugs applied for the clinical treatment of inflammatory diseases are glucocorticoids and NSAIDs that both push back inflammation by suppressing the biosynthesis of pro-inflammatory mediators such as cytokines, chemokines, and PGs [7,33,34]. But these mediators are crucial regulators of the normal immune response and/or play important roles in the homeostasis of the body, explaining why their suppression by drugs is afflicted with severe on-target side effects [7,35]. Moreover, the unwanted actions of NSAIDs are also due to substrate shunting to other LM routes, resulting in elevated LT levels due to redirection of AA for conversion by 5-LOX [8,36,37]. The discovery of the superfamily of SPM as LM that terminate inflammation and stimulate its

resolution, along with tissue repair and regeneration without being immunosuppressive, have prompted a paradigm shift in the view of inflammation pharmacotherapy [9,38]. There is accumulating evidence that many inflammation-related diseases might be connected to low SPM levels while elevating SPM in tissues, for example by exogenous application of SPM or supplementation of DHA and EPA, limits inflammation without immunosuppression and typical side effects of classical anti-inflammatory drugs [32,39]. In this respect, the chalcones MF-14 and MF-15 are able to elevate SPM levels as well as their precursors in human macrophages and could be of interest as potential candidates for further development as novel agents that promote the resolution of persistent and excessive inflammation.

Chalcones are polyphenolic compounds of the flavonoid family displaying antioxidant, oxygen scavenging, anti-inflammatory and anti-cancer activities [13,40,41]. Various natural and synthetic chalcones have been reported to reduce LT or PGE₂ levels [13], and their ability to inhibit 5-LOX activity was demonstrated for various structural derivatives using experimental models [14,42–46] supported also by *in silico* approaches [47,48]. However, stimulatory effects on SPM formation or on 12/15-LOX product formation have not been shown yet to the best of our knowledge, rather, inhibition of 15-LOX was reported for some hydroxychalcone-triazole hybrids [49]. Our previous unbiased *in silico* target prediction approach identified human 5-LOX as potential target of natural chalcones and dihydrochalcones, where we confirmed 5-LOX inhibition for phloretin and 3-OH-phloretin [15]. In the present study, we investigated MF-14 and MF-15 that are 2-OH-benzylated derivatives, which were identified as inhibitors of the androgen-synthesizing enzyme AKR1C3 [18]. Interestingly, in line with the inhibition of AKR1C3 [18], the dihydrochalcone MF-15 was consistently somewhat more effective versus the corresponding chalcone MF-14 for modulation of cellular LM biosynthesis. Both compounds inhibited the activity of isolated human recombinant

5-LOX in a cell-free assay in the one-digit micromolar range with comparable potency in A23187-activated human neutrophils that are known to substantially generate 5-LOX products including LTs under inflammatory conditions [50]. Inhibition of 5-LOX and suppression of LT formation by the chalcones was also evident in exotoxin-stimulated human MDM with either M1 or M2 phenotype, which are considered as adequate, biological relevant *in vitro* test systems for LM modulators [8]. The potency of the chalcones to inhibit 5-LOX activity in MDM was less pronounced as compared to PMNL and HEK293 cells, which might be due to potential differences in 5-LOX activation in the two cell types (e.g., Ca^{2+} and phosphorylation) under the distinct experimental conditions (e.g., different stimuli and incubation periods), as observed for other 5-LOX inhibitors before (Werz & Steinhilber *Biochem Pharmacol* 2005; Fischer L. *FASEB Journal* 2003). Moreover, when resting MDM were exposed to chalcones, even slight induction of modest 5-LOX product formation but no inhibition was obvious, possibly due to the accompanied elevated levels of free AA, potentially caused by cPLA₂ activation, but low catalytic turnover of 5-LOX where inhibitors might be less effective. Along these lines, the chalcones did not reduce the stimulus-induced release of AA or other PUFAs, excluding diminished substrate supply as reason for suppressed LT formation. In a definite experimental cell-based system, that is, A23187-activated HEK293 cells transfected with human recombinant 5-LOX [22], the chalcones were unequivocally identified as efficient 5-LOX inhibitors, regardless of the absence or presence of exogenous AA as substrate. Note that the inhibition of 5-LOX by the chalcones did not redirect AA to the COX pathway. Hence, the elevation of 12/15-LOX products by the chalcones is unlikely due to the well-known substrate shunting of 5-LOX inhibitors [51]. This is further supported by results with MF-15-treated M2-MDM that had been supplemented with exogenous PUFA, where the dihydrochalcone still enhanced SPM and 12/15-LOX product formation, despite ample supply of substrate.

It is intriguing that MF-14 and MF-15 failed to inhibit other LOXs but instead increased or even induced the activities of endogenous 15-LOX-1 in M2-MDM and of human recombinant 15-LOX-1 in HEK293 cells. Many other phenolic compounds that inhibit 5-LOX such as NDGA also interfere with 12/15-LOXs [10,52,53]. But some small molecule 5-LOX inhibitors including benzenesulfonamide-derivatives [54], ginkgolic acid [55], 3-*O*-acetyl-11-keto boswellic acid (AKBA) [10], the biflavanoid 8-methylscoetrin-4'-ol [56] and celastrol [11] were shown to enhance or the formation of 12-/15-LOX products including SPM in human neutrophils or macrophages or in inflamed murine peritoneal exudates. Among those compounds, only celastrol was found to induce 12/15-LOX product formation, albeit only up to approx. 5- or 2-fold in M2-MDM in absence or presence of exogenous PUFA, respectively [11], while the chalcones caused 70- or 50-fold elevations in this respect. Thus, the chalcones are considered effective activators of 15-LOX-1. Pronounced activation of 15-LOX-1 in M2-MDM without marked stimulation of 5-LOX and COX enzymes was observed also for the *S. aureus*-derived exotoxin α -hemolysin that mediates 15-LOX activation via its surface receptor ADAM10 [28]. In contrast to exotoxins [28], the ADAM10 inhibitor GI254023X (40 μ M) did not affect MF-15-induced LM formation (data not shown), excluding the involvement of ADAM10, as expected. Our experiments with HEK293 cells showed that 15-LOX-2 was less efficiently stimulated by MF-14 and MF-15, suggesting a certain degree of preference for the 15-LOX-1 isoform. Human M2-MDM strongly express 15-LOX-1 but hardly 15-LOX-2 [28], and 15-LOX-1 translocates to membranous structures in M2-MDM upon challenge with MF-14/MF-15, in analogy to treatment with α -hemolysin [28] or celastrol [11]. In fact, 12/15-LOX product formation in M1-MDM that express only the 15-LOX-2 but not the 15-LOX-1 isoform, was only moderately increased by MF-14 and MF-15. It should be noted that only the 15-LOX-1 isoform catalyzes oxygenation of AA and EPA at C12 or DHA at C14 position

[31,57], yielding 12-HETE and 12-HEPE or 14-HDHA, respectively, which were strongly elevated by the chalcones. Finally, prolonged exposure of MDM to the chalcones at concentrations that activated 15-LOX-1 (i.e., 3 to 10 μ M) for 24 or 48 h did neither affect cell viability nor MDM polarization and phenotype-selective expression of the LM-biosynthetic enzymes 5-LOX, 15-LOX-1 or COX-2, respectively.

In conclusion, the natural chalcones MF-14 and MF-15 efficiently stimulate 15-LOX-1 activity in M2-MDM and HEK293 cells for substantial LM formation. In biologically relevant cellular settings using human M2-MDM, the chalcones caused a favorable LM class shift related to inflammation: impaired formation of LT but elevated levels of SPM, which may reduce pro-inflammatory reactions but may govern resolution of inflammation and tissue regeneration. More comprehensive investigations in experimental and disease-relevant animal models may reveal the pharmacological potential of these compounds for anti-inflammatory pharmacotherapy.

5. Acknowledgment

This work was supported by the Deutsche Forschungsgemeinschaft (DFG), Collaborative Research Center SFB 1278 “PolyTarget”, projects A04, C01, C05 and Z01. The SEM facilities of the Jena Center for Soft Matter (JCSM) were also established with a grant from the German Science Foundation. V.T. is funded by the FWF Hertha Firnberg project T942. A.C.P. is funded by the RFI Objectif Végétal (Région Pays de la Loire) and FEDER. H.S. was funded by GECT Euregio Tirol–Südtirol–Trentino (IPN55). Apple tree leaves were provided to SONAS thanks to a collaboration with INRAE Angers (Marie-Noëlle BRISSET, Matthieu GAUCHER and Laurence Feugey).

Conflict of interest

The authors declare no conflict of interest.

Figure legends

Figure 1 The natural chalcone MF-14 and the dihydrochalcone MF-15 are cardamomin derivatives that inhibit human 5-lipoxygenase. (A) Chemical structures of MF-14 and MF-15. (B) Semi-synthesis of MF-15. i: HCl 1.25 N, MeOH, 90 °C, 3 h, 85%; ii: MOM-Br, diisopropylamine, dry THF, RT, 20 min, 54%; iii: methyl iodide, NaH 60%, THF, 0 °C, 1.5 h, 69%; iv: *p*TSA, DCM/EtOH 1/7, 60 °C, 1 h, 75%; v: 2-hydroxybenzyl alcohol, ZnCl₂, dioxane, MW 130 °C, 30 min, 60%. (C,D) Inhibition of 5-LOX activity by MF-14 and MF-15. (C) Isolated human recombinant 5-LOX was diluted in PBS containing EDTA (1 mM) and incubated with MF-14 or MF-15 at the indicated concentrations or vehicle (0.1% DMSO) for 10 min on ice. The samples were placed at 37 °C for 30 sec and then stimulated with 20 μM AA plus 2 mM CaCl₂ for 10 min at 37 °C. (D) Freshly isolated human PMNL (10⁷ cells per mL) were diluted in PBS containing 1 mM CaCl₂ and 0.1% glucose and incubated with MF-14 or MF-15 at the indicated concentrations or vehicle (0.1% DMSO) for 10 min at 37 °C and then stimulated with 2.5 μM A23187 for 10 min at 37 °C. After termination of the incubations, the formed lipid mediators were extracted by SPE and 5-LOX products were analyzed via RP-HPLC. Values are means ± SEM, given as percentage of vehicle control (= 100%), n=3.

Figure 2 Effects of MF-14 and MF-15 on LM profiles of exotoxin-stimulated M1- and M2-MDM and of LOX-transfected HEK-293 cells. (A,B) Human unpolarized MDM were kept in RPMI 1640 medium and incubated with MF-14 or MF-15 at the indicated concentrations or vehicle (0.1% DMSO) for 24 h at 37 °C and cell integrity and viability was assessed using (A) LDH release assay and (B) MTT assay, respectively. Values are means \pm SEM, given as percentage of vehicle control (= 100% integrity or viability), n=3. Statistics was performed via matched one-way ANOVA and Dunnett's multiple comparisons test against the DMSO control, * p<0.05. (C) M1-MDM and (D) M2-MDM (2×10^6 , each) were diluted in PBS containing 1 mM CaCl₂, incubated with vehicle (0.1% DMSO), MF-14 or MF-15 (10 μ M, each) for 10 min at 37 °C and stimulated with SACM (1%) for 180 min at 37 °C. Then, formed LM were extracted from the supernatants by SPE and analyzed by UPLC-MS/MS. Results are given as mean \pm SEM, presented as percentage of SACM-stimulated vehicle control (= 100%), n=5. Upper panels: grouped LM produced by 12/15-LOX, SPM, PUFA, 5-LOX and COX (according to Table1); middle panels: sum of ω -6-derived LM as indicated; lower panels: sum of ω -3-derived LM as indicated. (E) Stably LOX-transfected HEK293 cells (2×10^6 cells in 1 mL PBS containing 1 mM CaCl₂ and 0.1% glucose), were pre-incubated with vehicle (0.1% DMSO), MF-14 or MF-15 (10 μ M, each) for 15 min at 37 °C and then stimulated with 2.5 μ M ionophore A23187 plus 1 μ M AA at 37°C. Afterwards the reaction was stopped with ice-cold methanol and formed LMs were extracted by SPE and analyzed by UPLC-MS/MS. Results are given as mean \pm S.E.M in percentage versus vehicle control (= 100%) for 5-LOX-, 15-LOX-1-, and 15-LOX-2-transfected cells, n=3. Statistical analysis was performed via ratio-paired t-test, * p<0.05, ** p<0.01, *** p<0.001, **** p<0.0001.

Figure 3 MF-14 and MF-15 induce SPM biosynthesis and activate 15-LOX-1 in MDM. (A) M1-MDM and (B) M2-MDM (2×10^6 , each) were diluted in PBS containing 1 mM CaCl₂,

incubated with vehicle (0.1% DMSO), MF-14 or MF-15 (10 μ M, each) for 180 min at 37 °C. Then, formed LM were extracted from the supernatants by SPE and analyzed by UPLC-MS/MS. Results are given as mean \pm S.E.M., presented as percentage of vehicle-treated control (= 100%), n=5. Upper panels: grouped LM produced by 12/15-LOX, SPM, PUFA, 5-LOX and COX (according to Table1); middle panels: sum of ω -6-derived LM as indicated; lower panels: sum of ω -3-derived LM as indicated. Statistical analysis was performed via ratio-paired t-test, * p<0.05, ** p<0.01, *** p<0.001, **** p<0.0001. (C) M2-MDM (10⁶ cells in PBS plus 1 mM CaCl₂ and 5 mM MgCl₂) were incubated with MF-14 or MF-15 (10 μ M, each), SACM (1%) or vehicle (0.1% DMSO) for 180 min. Then, the cells were fixed, permeabilized, and incubated with antibodies against 5-LOX (red) and 15-LOX-1 (cyan blue). Immunofluorescence detection was determined via Zeiss Axiolab microscope; scale bars = 10 μ m. Results shown for one single cell are representative for approximately 100 individual cells analyzed in n=3 independent experiments with separate donors, each.

Figure 4 MF-14 and MF-15 induce 15-LOX-1-related LM formation in HEK293 cells.

HEK293 cells (2 \times 10⁶ cells in 1 mL PBS containing 1 mM CaCl₂ plus 0.1% glucose) were incubated with AA, EPA, and DHA (1 μ M, each) plus vehicle (0.1 % DMSO) or MF-14 or MF-15 (10 μ M, each) for 180 min at 37 °C. Then, formed LMs were extracted by SPE and analyzed by UPLC-MS/MS. Results (mean of n=3 experiments) are given as -fold increase versus vehicle-treated control cells (= 100%) in a heatmap.

Figure 5 Effects of MF-14 and MF-15 on macrophage surface markers and the protein level of LM-biosynthetic enzymes during MDM polarization. (A) Unpolarized MDM were treated


with MF14 or MF15 (3 μ M, each) or 0.1% DMSO as vehicle. After 48 h, expression of the surface markers CD54 and CD80 (M1-like) as well as CD163 and CD206 (M2-like) among living CD14⁺ cells was analyzed by flow cytometry. Upper panel: shown are representative pseudocolor dot plots of the surface markers. Mean fluorescence intensity (MFI) of each marker was determined. Lower panel: the change of the MFI from MF14- and MF15-treated MDM against the MFI of DMSO-treated cells (control) was calculated and is given in % of control in scatter dot plots as single values and means \pm S.E.M., n=3. Statistics are calculated with raw data (MFI), * $p < 0.05$ MF14 vs. control group, ratio paired t-test. **(B)** Unpolarized MDM were incubated with MF-14 or MF-15 (10 μ M, each) for 48 h during the polarization process to M1- or M2-MDM. Cell lysates were prepared and immunoblotted for expression of 5-LOX, 15-LOX-2 and COX-2 in M1-MDM and of 5-LOX and 15-LOX-1 in M2-MDM, followed by densitometric analysis against β -actin (for normalization). Data are shown as mean \pm S.E.M, n= 3-5. Statistical analysis was performed via ratio-paired t-test.

Table 1 MF-14 and MF-15 modulate LM profiles of exotoxin-stimulated M1- and M2-MDM.

M1- and M2-MDM (2×10^6 cells, each) were preincubated in PBS containing 1 mM CaCl₂ with vehicle (0.1% DMSO), MF-14 or MF-15 (10 μ M, each) for 10 min at 37 °C and then stimulated with SACM (1%) for 180 min at 37 °C. Formed LM in the supernatants were analyzed by UPLC-MS/MS. Results are given in pg/ 2×10^6 cells as means \pm SEM and as -fold change versus SACM-stimulated vehicle control (ctrl. = 1) in a heatmap, n=5. Results below the limit of quantification are indicated as non-quantifiable (n.q.).

		M1 ctrl			MF-14 [10 μ M]			M1 ctrl			MF-15 [10 μ M]			M2 ctrl			MF-14 [10 μ M]			M2 ctrl			MF-15 [10 μ M]		
				-fold			-fold			-fold			-fold			-fold			-fold			-fold			
5-LOX	5-HEPE	416 \pm 148	240 \pm 183	0.6	289 \pm 74	110 \pm 33	0.4	247 \pm 36	169 \pm 43	0.7	445 \pm 98	182 \pm 60	0.4												
	5-HETE	3590 \pm 1757	1325 \pm 380	0.4	2710 \pm 1244	1183 \pm 580	0.4	2759 \pm 462	1704 \pm 274	0.6	6452 \pm 2550	2364 \pm 648	0.4												
	1-LTB ₄	283 \pm 111	142 \pm 111	0.5	244 \pm 65	77 \pm 32	0.3	332 \pm 26	186 \pm 36	0.6	731 \pm 272	222 \pm 70	0.3												
	LTB ₄	1387 \pm 572	867 \pm 943	0.6	1310 \pm 470	267 \pm 129	0.2	609 \pm 101	461 \pm 108	0.8	1655 \pm 737	391 \pm 108	0.2												
COX	5S,6R-dihETE	145 \pm 72	70 \pm 51	0.5	119 \pm 54	42 \pm 23	0.3	121 \pm 8	90 \pm 18	0.7	357 \pm 152	104 \pm 32	0.3												
	PGE ₂	6251 \pm 4286	5543 \pm 6450	0.9	1962 \pm 506	2627 \pm 578	1.3	354 \pm 91	601 \pm 213	1.7	249 \pm 36	337 \pm 54	1.4												
	PGD ₂	85 \pm 25	107 \pm 33	1.3	38 \pm 3	73 \pm 15	1.9	75 \pm 27	110 \pm 46	1.5	46 \pm 8	63 \pm 17	1.4												
	PGF _{2α}	822 \pm 280	765 \pm 564	0.9	474 \pm 105	522 \pm 79	1.1	220 \pm 109	325 \pm 208	1.5	100 \pm 23	130 \pm 32	1.3												
12/15-LOX	TXB ₂	17936 \pm 6018	12400 \pm 10781	0.7	10165 \pm 1203	8963 \pm 1219	0.9	10668 \pm 4323	7162 \pm 4038	0.7	5301 \pm 1354	4984 \pm 1779	0.9												
	17-HDHA	926 \pm 237	1697 \pm 264	1.8	510 \pm 171	1276 \pm 384	2.5	5986 \pm 2970	11486 \pm 6004	1.9	2906 \pm 1255	5075 \pm 1151	1.7												
	14-HDHA	168 \pm 38	118 \pm 19	0.7	140 \pm 26	107 \pm 34	0.8	1467 \pm 521	2846 \pm 1710	1.9	719 \pm 146	1208 \pm 238	1.7												
	7-HDHA	116 \pm 22	75 \pm 47	0.6	86 \pm 20	42 \pm 3	0.5	286 \pm 112	397 \pm 181	1.4	184 \pm 29	202 \pm 45	1.1												
SPMs	4-HDHA	89 \pm 16	90 \pm 10	1.0	63 \pm 11	72 \pm 14	1.1	88 \pm 19	95 \pm 26	1.1	94 \pm 13	90 \pm 11	1.0												
	15-HEPE	91 \pm 19	174 \pm 32	1.9	61 \pm 17	124 \pm 30	2.0	816 \pm 405	2553 \pm 1448	3.1	351 \pm 155	801 \pm 198	2.3												
	12-HEPE	51 \pm 12	34 \pm 14	0.7	54 \pm 13	71 \pm 25	1.3	207 \pm 74	475 \pm 251	2.3	116 \pm 16	178 \pm 35	1.5												
	15-HETE	1552 \pm 134	3276 \pm 706	2.1	930 \pm 162	3088 \pm 678	3.3	9654 \pm 4569	21506 \pm 8179	2.2	3979 \pm 1132	12835 \pm 3561	3.2												
PUFA	12-HETE	857 \pm 359	282 \pm 250	0.3	449 \pm 207	1028 \pm 377	2.3	1679 \pm 484	4188 \pm 1967	2.5	1703 \pm 609	2236 \pm 745	1.3												
	5,15-dihETE	105 \pm 46	61 \pm 65	0.6	52 \pm 6	28 \pm 4	0.5	900 \pm 570	1781 \pm 1211	2.0	384 \pm 143	619 \pm 290	1.6												
	PD1	3.0 \pm 0.7	4.7 \pm 0.4	1.5	2.0 \pm 0.6	4.1 \pm 2.3	2.0	17 \pm 7	32 \pm 16	1.9	10 \pm 2	18 \pm 7	1.8												
	PDX	8.0 \pm 3.3	15.9 \pm 1.8	2.0	5.5 \pm 2.7	13.7 \pm 8.0	2.5	31 \pm 9	55 \pm 17	1.8	31 \pm 9	60 \pm 25	1.9												
PUFA	RvD5	8.9 \pm 3.1	5.6 \pm 3.7	0.6	5.8 \pm 1.8	2.8 \pm 0.4	0.5	368 \pm 252	733 \pm 490	2.0	106 \pm 62	190 \pm 93	1.8												
	MaR1	5.9 \pm 2.4	2.7 \pm 2.9	0.5	2.5 \pm 1.6	3.4 \pm 2.2	1.3	33 \pm 9	46 \pm 11	1.4	23 \pm 10	34 \pm 15	1.5												
	AA	632322 \pm 294318	813832 \pm 585167	1.3	486287 \pm 215813	722736 \pm 355550	1.5	708077 \pm 325600	881911 \pm 480958	1.2	592316 \pm 302582	736718 \pm 381686	1.2												
	EPA	229764 \pm 101624	315238 \pm 213017	1.4	174013 \pm 82639	291918 \pm 148084	1.7	240368 \pm 121104	309628 \pm 172659	1.3	227858 \pm 124036	266763 \pm 154736	1.2												
DHA	174632 \pm 34609	231448 \pm 68947	1.3	160498 \pm 32651	176109 \pm 44458	1.1	183458 \pm 43893	184596 \pm 59792	1.0	151096 \pm 44656	173852 \pm 53984	1.2													

Table 2 MF-14 and MF-15 modulate ionophore A23187-induced LM formation in LOX-transfected HEK293 cells. Stably LOX-transfected HEK293 cells (2×10^6 cells in 1 mL PBS containing 1 mM CaCl_2 and 0.1% glucose), were pre-incubated with vehicle (0.1% DMSO), MF-14 or MF-15 (10 μM , each) for 15 min at 37 °C and then stimulated with 2.5 μM ionophore A23187 plus 1 μM AA at 37 °C. Afterwards, the reaction was stopped with ice-cold methanol and formed LMs were extracted by SPE and analyzed by UPLC-MS/MS. Results are given in pg/ 2×10^6 cells as means \pm S.E.M and as -fold change versus ionophore-stimulated vehicle control (ctrl. = 1) in a heatmap, n=3.



	LM	DMSO	MF-14		MF-15	
			pg/ 2×10^6 cells	-fold	pg/ 2×10^6 cells	-fold
5-LOX	5-HEPE	119 \pm 15	16 \pm 11	0.1	30 \pm 24	0.2
	5-HETE	11913 \pm 5492	712 \pm 59	0.1	754 \pm 72	0.1
	t-LTB ₄	759 \pm 359	15 \pm 5	0.0	11 \pm 1	0.0
	LTB ₄	1180 \pm 538	16 \pm 3	0.0	14 \pm 3	0.0
	17-HDHA	40 \pm 31	49 \pm 24	1.2	92 \pm 75	2.3
	14-HDHA	13.6 \pm 9.3	14.3 \pm 9.1	1.1	18.9 \pm 13.5	1.4
	15-HEPE	6.8 \pm 2.3	9.6 \pm 3.7	1.4	9.3 \pm 4.5	1.4
	15-HETE	434 \pm 54	589 \pm 219	1.4	501 \pm 92	1.2
15-LOX-1	5-HEPE	3.4 \pm 0.2	3.8 \pm 0.3	1.1	3.5 \pm 0.4	1.0
	5-HETE	246 \pm 120	202 \pm 67	0.8	273 \pm 102	1.1
	t-LTB ₄	4.9 \pm 0.3	6.9 \pm 2.5	1.4	12.2 \pm 3.6	2.5
	LTB ₄	4.8 \pm 1.3	5.5 \pm 1.4	1.2	10.9 \pm 4.0	2.3
	17-HDHA	55 \pm 35	116 \pm 85	2.1	181 \pm 111	3.3
	14-HDHA	16 \pm 9	40 \pm 21	2.5	55 \pm 32	3.4
	15-HEPE	21 \pm 13	34 \pm 24	1.6	54 \pm 33	2.6
	15-HETE	1699 \pm 1356	1539 \pm 1124	0.9	2542 \pm 1911	1.5
15-LOX-2	5-HEPE	4.8 \pm 1.1	3.4 \pm 0.7	0.7	3.3 \pm 0.5	0.7
	5-HETE	320 \pm 172	136 \pm 35	0.4	167 \pm 29	0.5
	t-LTB ₄	14.2 \pm 7.5	3.9 \pm 1.2	0.3	5.9 \pm 1.7	0.4
	LTB ₄	10.9 \pm 4.9	2.2 \pm 0.9	0.2	4.5 \pm 2.1	0.4
	17-HDHA	1473 \pm 377	1708 \pm 377	1.2	1865 \pm 485	1.3
	14-HDHA	12 \pm 2	13 \pm 2	1.1	15 \pm 2	1.3
	15-HEPE	646 \pm 137	549 \pm 113	0.9	504 \pm 113	0.8
	15-HETE	9779 \pm 4302	10407 \pm 3092	1.1	10566 \pm 4593	1.1

Table 3 MF-14 and MF-15 induce LM formation in M1- and M2-MDM. M1- and M2-MDM (2×10^6 cells in 1 mL PBS containing 1 mM CaCl_2) were incubated with vehicle (0.1 % DMSO) or with MF-14 or MF-15 (10 μM) for 180 min at 37 °C. Formed LM in the supernatants were analyzed by UPLC-MS/MS. Results are given in pg/ 2×10^6 cells as means \pm S.E.M and as -fold change versus unstimulated vehicle control (ctrl. = 1) in a heatmap, n=5. For results below the limit of quantification, LM are indicated as non-quantifiable (n.q.), and the limit of quantification was used as basis for -fold change calculation.

		0		1		60		M1 MDM					M2 MDM										
		DMSO		MF-14		-fold		DMSO		MF-15		-fold		DMSO		MF-14		DMSO		MF-15		-fold	
5-LOX	5-HEPE	8.1 \pm 1.3	19.4 \pm 2.3	2.4	5.3 \pm 0.5	15.1 \pm 2.8	2.8	5.4 \pm 0.9	23.1 \pm 3.2	4.2	8.3 \pm 3.3	22.4 \pm 3.9	2.7										
	5-HETE	61.7 \pm 23.3	122 \pm 37	2.0	35.1 \pm 9.5	120 \pm 32	3.4	25.3 \pm 5.8	140 \pm 36	5.5	36.7 \pm 12.7	189 \pm 53	5.1										
	1-LTB ₄	17.1 \pm 6.9	14.9 \pm 5.8	0.9	6.8 \pm 2.2	9.9 \pm 1.1	1.4	6.4 \pm 3.7	13.0 \pm 3.3	2.0	5.8 \pm 3.0	20.7 \pm 7.7	3.5										
	LTB ₄	11.5 \pm 4.2	24.5 \pm 6.7	2.1	4.6 \pm 1.1	11.1 \pm 3.6	2.4	5.6 \pm 2.1	13.8 \pm 3.8	2.5	4.8 \pm 1.8	25.5 \pm 10.9	5.3										
COX	5S,6R-dihETE	1.8 \pm 0.3	3.9 \pm 1.1	2.2	1.3 \pm 0.4	3.3 \pm 0.2	2.5	0.5 \pm 0.3	2.1 \pm 0.5	3.8	0.6 \pm 0.2	3.1 \pm 1.5	5.0										
	PGE ₂	1505 \pm 610	752 \pm 202	0.5	546 \pm 168	561 \pm 212	1.0	34.9 \pm 7.2	60 \pm 16	1.7	36.9 \pm 6.4	72 \pm 12	1.9										
	PGD ₂	23.8 \pm 8.6	25.6 \pm 8.1	1.1	11.3 \pm 2.7	16.8 \pm 6.0	1.5	6.8 \pm 1.6	9.7 \pm 1.6	1.4	9.8 \pm 1.6	13 \pm 0	1.3										
	PGF _{2α}	560 \pm 239	349 \pm 176	0.6	205 \pm 50	158 \pm 52	0.8	19.0 \pm 3.1	21.4 \pm 6.3	1.1	20.4 \pm 4.7	38 \pm 16	1.9										
12/15-LOX	TXB ₂	6731 \pm 1720	3769 \pm 808	0.6	3168 \pm 617	2354 \pm 703	0.7	378 \pm 82	304 \pm 71	0.8	533 \pm 129	1166 \pm 693	2.2										
	17-HDHA	76.1 \pm 20.8	581 \pm 420	7.6	37.9 \pm 5.5	195 \pm 73	5.1	33.7 \pm 8.0	967 \pm 455	28.7	46.0 \pm 10.2	696 \pm 195	15.1										
	14-HDHA	41.6 \pm 13.7	159.1 \pm 73.5	3.8	6.3 \pm 0.7	37.5 \pm 9.8	5.9	9.4 \pm 1.5	329 \pm 157	34.8	14.4 \pm 3.5	244 \pm 86	17.0										
	7-HDHA	18.0 \pm 3.5	15.9 \pm 3.0	0.9	10.5 \pm 1.8	14.7 \pm 2.5	1.4	12.0 \pm 4.1	55.1 \pm 23.7	4.6	9.8 \pm 2.6	38.4 \pm 8.3	3.9										
	4-HDHA	13.7 \pm 3.4	31.9 \pm 4.5	2.3	9.0 \pm 1.6	27.1 \pm 8.0	3.0	10.6 \pm 2.3	47.7 \pm 10.0	4.5	15.0 \pm 4.6	60.8 \pm 10.9	4.1										
	15-HEPE	13.7 \pm 3.1	59.2 \pm 38.6	4.3	5.9 \pm 0.9	19.3 \pm 4.6	3.3	6.2 \pm 0.8	123 \pm 55	19.9	7.6 \pm 1.7	74.0 \pm 19.7	9.7										
	12-HEPE	8.9 \pm 4.0	33.4 \pm 6.4	3.8	3.4 \pm 0.4	16.6 \pm 3.9	4.8	3.6 \pm 0.8	63.7 \pm 28.2	17.6	5.0 \pm 1.4	107 \pm 63	21.4										
	15-HETE	94.8 \pm 31.2	1167 \pm 907	12.3	51.5 \pm 12.6	385 \pm 152	7.5	20.9 \pm 2.9	1934 \pm 906	52.3	35.7 \pm 13.9	1467 \pm 486	41.1										
	12-HETE	241 \pm 212	557 \pm 263	2.3	27 \pm 4	194 \pm 66	7.3	19.9 \pm 2.6	713 \pm 374	35.8	28.5 \pm 11.0	1783 \pm 903	62.5										
	5,15-dihETE	38.6 \pm 12.6	11.7 \pm 1.8	0.3	12.5 \pm 4.1	10.4 \pm 1.6	0.8	10.1 \pm 4.4	47.1 \pm 30.5	4.6	6.0 \pm 2.3	25.1 \pm 12.9	4.2										
SPMs	PD1	0.8 \pm 0.3	1.3 \pm 0.3	1.5	1.0 \pm 0.2	0.9 \pm 0.2	1.0	0.9 \pm 0.1	2.3 \pm 0.7	2.6	0.8 \pm 0.1	1.4 \pm 0.3	1.8										
	PDX	2.1 \pm 0.4	4.1 \pm 0.8	1.9	1.9 \pm 0.1	2.6 \pm 0.3	1.4	2.2 \pm 0.4	4.3 \pm 1.0	2.0	2.3 \pm 0.4	4.6 \pm 1.1	2.0										
	RvD5	2.0 \pm 0.8	2.1 \pm 0.7	1.0	1.4 \pm 0.5	1.5 \pm 0.3	1.1	1.8 \pm 0.9	35.8 \pm 21.0	19.9	1.9 \pm 0.5	15.6 \pm 8.9	8.2										
	MaR1	2.9 \pm 2.2	1.7 \pm 1.1	0.6	3.1 \pm 1.8	1.7 \pm 1.4	0.6	2.2 \pm 1.7	8.7 \pm 5.4	3.9	2.2 \pm 1.8	3.6 \pm 2.2	1.7										
PUFA	AA	36894 \pm 17530	362368 \pm 295912	9.8	24292 \pm 12653	254992 \pm 205073	10.5	22004 \pm 7943	284347 \pm 174831	12.9	29361 \pm 8529	310294 \pm 192949	10.6										
	EPA	6181 \pm 3342	113524 \pm 99337	18.4	3827 \pm 1789	43073 \pm 32916	11.3	2577 \pm 751	55025 \pm 31217	21.4	4518 \pm 1624	62506 \pm 34402	13.8										
	DHA	28662 \pm 8325	81260 \pm 37528	2.8	14467 \pm 2608	51858 \pm 23877	3.6	16391 \pm 2923	93140 \pm 22434	5.7	25228 \pm 5947	102093 \pm 25346	4.0										

Table 4 MF-14 and MF-15 induce LM formation in M1- and M2-MDM in the presence of exogenous PUFA. M1- and M2-MDM (2×10^6 cells in 1 mL PBS containing 1 mM CaCl_2) were incubated with vehicle (0.1 % DMSO) or with MF-14 or MF-15 (10 μM), all samples received AA, EPA and DHA (1 μM , each). After 180 min at 37 °C, formed LM in the supernatants were analyzed by UPLC-MS/MS. Results are given in pg/ 2×10^6 cells as means \pm S.E.M and as -fold change versus unstimulated vehicle control (ctrl. = 1) that received only the PUFAs in a heatmap, n=3. For results below the limit of quantification, LM are indicated as non-quantifiable (n.q.), and the limit of quantification was used as basis for -fold change calculation.

		M2 MDM					
		DMSO	MF-14	-fold	MF-15	-fold	
5-LOX	5-HEPE	345 \pm 190	1245 \pm 74	3.6	1025 \pm 77	3.0	
	5-HETE	122 \pm 59	664 \pm 97	5.5	782 \pm 84	6.4	
	t-LTB ₄	4.6 \pm 1.2	13.5 \pm 4.6	3.0	21.9 \pm 7.0	4.8	
	LTB ₄	1.7 \pm 0.3	26.2 \pm 8.5	15.9	31.2 \pm 10.7	18.9	
	5S,6R-diHETE	1.9 \pm 1.0	5.8 \pm 1.7	3.0	8.3 \pm 2.7	4.3	
COX	PGE ₂	90 \pm 10	92 \pm 18	1.0	110 \pm 18	1.2	
	PGD ₂	72 \pm 23	72 \pm 19	1.0	86 \pm 16	1.2	
	PGF _{2α}	41 \pm 11	48 \pm 13	1.2	58 \pm 17	1.4	
	TXB ₂	315 \pm 65	169 \pm 27	0.5	240 \pm 44	0.8	
12/15-LOX	17-HDHA	222 \pm 74	2784 \pm 111	12.5	2213 \pm 62	10.0	
	14-HDHA	40 \pm 15	361 \pm 55	9.1	316 \pm 69	7.9	
	7-HDHA	100 \pm 29	332 \pm 36	3.3	302 \pm 25	3.0	
	4-HDHA	172 \pm 65	688 \pm 106	4.0	689 \pm 85	4.0	
	15-HEPE	77.2 \pm 33.4	3043 \pm 507	39.4	2630 \pm 226	34.1	
	12-HEPE	48.0 \pm 27.4	748 \pm 71	15.6	800 \pm 113	16.7	
	15-HETE	80.4 \pm 33.2	4493 \pm 324	55.9	4353 \pm 505	54.1	
12-HETE	33.7 \pm 10.5	391 \pm 24	11.6	475 \pm 75	14.1		
5,15-diHETE	168 \pm 37	92 \pm 17	0.5	83 \pm 4	0.5		
SPMs	PD1	7.7 \pm 1.0	12.2 \pm 2.2	1.6	17.6 \pm 1.0	2.3	
	PDX	7.8 \pm 1.0	35.3 \pm 1.9	4.5	33.5 \pm 1.5	4.3	
	RvD5	3.7 \pm 1.0	41.3 \pm 11.0	11.1	49.1 \pm 8.7	13.3	
	MaR1	0.7 \pm 0.1	6.6 \pm 1.1	9.1	7.1 \pm 0.3	9.8	
PUFA	AA	283014 \pm 75653	1260910 \pm 140332	4.5	1183611 \pm 41237	4.2	
	EPA	322106 \pm 54447	750468 \pm 72546	2.3	681909 \pm 8675	2.1	
	DHA	143001 \pm 40219	471581 \pm 39321	3.3	434404 \pm 8555	3.0	

+ 1 μM (AA, EPA and DHA)

References

- [1] C.N. Serhan, J. Savill, Resolution of inflammation: The beginning programs the end, *Nature Immunology*. 6 (2005) 1191–1197. <https://doi.org/10.1038/ni1276>.
- [2] C. Funk, Prostaglandins and leukotrienes: Advances in eicosanoid biology, *Science*. 294 (2001) 1871–1875. <https://doi.org/10.1126/science.294.5548.1871>.
- [3] R.A. Whittington, E. Planel, N. Terrando, Impaired resolution of inflammation in Alzheimer's disease: A review, *Frontiers in Immunology*. 8 (2017). <https://doi.org/10.3389/fimmu.2017.01464>.
- [4] R. Medzhitov, Inflammation 2010: New Adventures of an Old Flame, *Cell*. 140 (2010) 771–776. <https://doi.org/10.1016/j.cell.2010.03.006>.
- [5] C.D. Buckley, D.W. Gilroy, C.N. Serhan, Proresolving lipid mediators and mechanisms in the resolution of acute inflammation, *Immunity*. 40 (2014) 315–327. <https://doi.org/10.1016/j.immuni.2014.02.009>.
- [6] C.N. Serhan, Pro-resolving lipid mediators are leads for resolution physiology, *Nature*. 510 (2014) 92–101. <https://doi.org/10.1038/nature13479>.
- [7] K.D. Rainsford, Anti-inflammatory drugs in the 21st century., *Sub-Cellular Biochemistry*. 42 (2007) 3–27. https://doi.org/10.1007/1-4020-5688-5_1.
- [8] M. Werner, P.M. Jordan, E. Romp, A. Czapka, Z. Rao, C. Kretzer, A. Koeberle, U. Garscha, S. Pace, H.E. Claesson, C.N. Serhan, O. Werz, J. Gerstmeier, Targeting biosynthetic networks of the proinflammatory and proresolving lipid metabolome, *FASEB Journal : Official Publication of the Federation of American Societies for Experimental Biology*. 33 (2019) 6140–6153. <https://doi.org/10.1096/fj.201802509R>.

- [9] C.N. Serhan, B.D. Levy, Resolvins in inflammation: Emergence of the pro-resolving superfamily of mediators, *Journal of Clinical Investigation*. 128 (2018) 2657–2669. <https://doi.org/10.1172/JCI97943>.
- [10] N.C. Gilbert, J. Gerstmeier, E.E. Schexnaydre, F. Börner, U. Garscha, D.B. Neau, O. Werz, M.E. Newcomer, Structural and mechanistic insights into 5-lipoxygenase inhibition by natural products, *Nature Chemical Biology*. 16 (2020) 783–790. <https://doi.org/10.1038/s41589-020-0544-7>.
- [11] S. Pace, K. Zhang, P.M. Jordan, R. Bilancia, W. Wang, F. Börner, R.K. Hofstetter, M. Potenza, C. Kretzer, J. Gerstmeier, D. Fischer, S. Lorkowski, N.C. Gilbert, M.E. Newcomer, A. Rossi, X. Chen, O. Werz, Anti-inflammatory celastrol promotes a switch from leukotriene biosynthesis to formation of specialized pro-resolving lipid mediators, *Pharmacological Research*. 167 (2021). <https://doi.org/10.1016/j.phrs.2021.105556>.
- [12] G. Di Carlo, N. Mascolo, A.A. Izzo, F. Capasso, Flavonoids: Old and new aspects of a class of natural therapeutic drugs, *Life Sciences*. 65 (1999) 337–353. [https://doi.org/10.1016/S0024-3205\(99\)00120-4](https://doi.org/10.1016/S0024-3205(99)00120-4).
- [13] A. V. Mahapatra DK, Bharti SK, Chalcone Derivatives: Anti-inflammatory Potential and Molecular Targets Perspectives., *Curr Top Med Chem*. 20;17(28) (2017) 3146–3169. <https://doi.org/10.2174/1568026617666170914160446>.
- [14] F. Herencia, M.L. Ferrándiz, A. Ubeda, J.N. Domínguez, J.E. Charris, G.M. Lobo, M.J. Alcaraz, Synthesis and anti-inflammatory activity of chalcone derivatives, *Bioorganic and Medicinal Chemistry Letters*. (1998). [https://doi.org/10.1016/S0960-894X\(98\)00179-6](https://doi.org/10.1016/S0960-894X(98)00179-6).
- [15] F. Mayr, G. Möller, U. Garscha, J. Fischer, P.R. Castaño, S.G. Inderbinen, V. Temml, B. Waltenberger, S. Schwaiger, R.W. Hartmann, C. Gege, S. Martens, A. Odermatt, A. V.

- Pandey, O. Werz, J. Adamski, H. Stuppner, D. Schuster, Finding new molecular targets of familiar natural products using in silico target prediction, *International Journal of Molecular Sciences*. 21 (2020) 1–18. <https://doi.org/10.3390/ijms21197102>.
- [16] Z.H. Huang, L.Q. Yin, L.P. Guan, Z.H. Li, C. Tan, Screening of chalcone analogs with anti-depressant, anti-inflammatory, analgesic, and COX-2-inhibiting effects, *Bioorganic and Medicinal Chemistry Letters*. 30 (2020) 127173. <https://doi.org/10.1016/j.bmcl.2020.127173>.
- [17] S.E. Kovar, C. Fourman, C. Kinstedt, B. Williams, C. Morris, K. jin Cho, D.M. Ketcha, Chalcones bearing a 3,4,5-trimethoxyphenyl motif are capable of selectively inhibiting oncogenic K-Ras signaling, *Bioorganic and Medicinal Chemistry Letters*. 30 (2020) 127144. <https://doi.org/10.1016/j.bmcl.2020.127144>.
- [18] M. Kafka, F. Mayr, V. Temml, G. Möller, J. Adamski, J. Höfer, S. Schwaiger, I. Heidegger, B. Matuszczak, D. Schuster, H. Klocker, J. Bektic, H. Stuppner, I.E. Eder, Dual inhibitory action of a novel akr1c3 inhibitor on both full-length ar and the variant AR-V7 in enzalutamide resistant metastatic castration resistant prostate cancer, *Cancers*. 12 (2020) 1–18. <https://doi.org/10.3390/cancers12082092>.
- [19] R.B. Filho, M.S. da Silva, O.R. Gottlieb, Flavonoids from *Iryanthera laevis*, *Phytochemistry*. 19 (1980). [https://doi.org/10.1016/0031-9422\(80\)83082-2](https://doi.org/10.1016/0031-9422(80)83082-2).
- [20] U. Prawat, O. Chairerk, U. Phupornprasert, A.-W. Salae, P. Tuntiwachwuttikul, Two New C-benzylated Dihydrochalcone Derivatives from the Leaves of *Melodorum siamensis*, *Planta Medica*. 79 (2012). <https://doi.org/10.1055/s-0032-1327950>.
- [21] O. Werz, J. Gerstmeier, S. Libreros, X. de La Rosa, M. Werner, P.C. Norris, N. Chiang, C.N. Serhan, Human macrophages differentially produce specific resolvin or leukotriene

signals that depend on bacterial pathogenicity, *Nature Communications*. 9 (2018) 1–12.
<https://doi.org/10.1038/s41467-017-02538-5>.

- [22] J. Gerstmeier, C. Weinigel, D. Barz, O. Werz, U. Garscha, An experimental cell-based model for studying the cell biology and molecular pharmacology of 5-lipoxygenase-activating protein in leukotriene biosynthesis, *Biochimica et Biophysica Acta - General Subjects*. 1840 (2014) 2961–2969. <https://doi.org/10.1016/j.bbagen.2014.05.016>.
- [23] L. Fischer, D. Szellas, O. Rådmark, D. Steinhilber, O. Werz, Phosphorylation- and stimulus-dependent inhibition of cellular 5-lipoxygenase activity by nonredox-type inhibitors., *The FASEB Journal: Official Publication of the Federation of American Societies for Experimental Biology*. 17 (2003) 949–951. <https://doi.org/10.1096/fj.02-0815fje>.
- [24] D. Steinhilber, T. Herrmann, H.J. Roth, Separation of lipoxins and leukotrienes from human granulocytes by high-performance liquid chromatography with a Radial-Pak cartridge after extraction with an octadecyl reversed-phase column, *Journal of Chromatography B: Biomedical Sciences and Applications*. 493 (1989) 361–366.
[https://doi.org/10.1016/S0378-4347\(00\)82742-5](https://doi.org/10.1016/S0378-4347(00)82742-5).
- [25] B. Shkodra-Pula, C. Kretzer, P.M. Jordan, P. Klemm, A. Koeberle, D. Pretzel, E. Banoglu, S. Lorkowski, M. Wallert, S. Höppener, S. Stumpf, A. Vollrath, S. Schubert, O. Werz, U.S. Schubert, Encapsulation of the dual FLAP/mPEGS-1 inhibitor BRP-187 into acetalated dextran and PLGA nanoparticles improves its cellular bioactivity, *Journal of Nanobiotechnology*. 18 (2020) 73. <https://doi.org/10.1186/s12951-020-00620-7>.
- [26] L. Thomas, Z. Rao, J. Gerstmeier, M. Raasch, C. Weinigel, S. Rummler, D. Menche, R. Müller, C. Pergola, A. Mosig, O. Werz, Selective upregulation of TNF α expression in classically-activated human monocyte-derived macrophages (M1) through pharmacological

- interference with V-ATPase, *Biochemical Pharmacology*. 130 (2017) 71–82. <https://doi.org/10.1016/j.bcp.2017.02.004>.
- [27] O. Werz, E. Bürkert, B. Samuelsson, O. Rådmark, D. Steinhilber, Activation of 5-lipoxygenase by cell stress is calcium independent in human polymorphonuclear leukocytes, *Blood*. 99 (2002) 1044–1052. <https://doi.org/10.1182/blood.V99.3.1044>.
- [28] P.M. Jordan, J. Gerstmeier, S. Pace, R. Bilancia, Z. Rao, F. Börner, L. Miek, Ó. Gutiérrez-Gutiérrez, V. Arakandy, A. Rossi, A. Ialenti, C. González-Estévez, B. Löffler, L. Tuchscher, C.N. Serhan, O. Werz, Staphylococcus aureus-Derived α -Hemolysin Evokes Generation of Specialized Pro-resolving Mediators Promoting Inflammation Resolution, *Cell Reports*. 33 (2020). <https://doi.org/10.1016/j.celrep.2020.108247>.
- [29] A. Gupte, J.K. Buolamwini, Synthesis and biological evaluation of phloridzin analogs as human concentrative nucleoside transporter 3 (hCNT3) inhibitors, *Bioorganic & Medicinal Chemistry Letters*. 19 (2009). <https://doi.org/10.1016/j.bmcl.2008.11.112>.
- [30] S. Urgaonkar, H.S. la Pierre, I. Meir, H. Lund, D. RayChaudhuri, J.T. Shaw, Synthesis of Antimicrobial Natural Products Targeting FtsZ: (\pm)-Dichamanetin and (\pm)-2'-Hydroxy-5'-benzylisouvarinol-B, *Organic Letters*. 7 (2005). <https://doi.org/10.1021/ol052269z>.
- [31] I. Ivanov, H. Kuhn, D. Heydeck, Structural and functional biology of arachidonic acid 15-lipoxygenase-1 (ALOX15), *Gene*. 573 (2015) 1–32. <https://doi.org/10.1016/j.gene.2015.07.073>.
- [32] J. Dalli, C.N. Serhan, Identification and structure elucidation of the pro-resolving mediators provides novel leads for resolution pharmacology., *British Journal of Pharmacology*. 176 (2019) 1024–1037. <https://doi.org/10.1111/bph.14336>.

- [33] C.A. Dinarello, Anti-inflammatory Agents: Present and Future., *Cell*. 140 (2010) 935–50. <https://doi.org/10.1016/j.cell.2010.02.043>.
- [34] T. Hanke, D. Merk, D. Steinhilber, G. Geisslinger, M. Schubert-Zsilavecz, Small molecules with anti-inflammatory properties in clinical development, *Pharmacology and Therapeutics*. 157 (2016) 163–187. <https://doi.org/10.1016/j.pharmthera.2015.11.011>.
- [35] P.J. Barnes, Glucocorticosteroids., *Handbook of Experimental Pharmacology*. 237 (2017) 93–115. https://doi.org/10.1007/164_2016_62.
- [36] K. Yang, W. Ma, H. Liang, Q. Ouyang, C. Tang, L. Lai, Dynamic simulations on the arachidonic acid metabolic network, *PLoS Computational Biology*. 3 (2007) 0523–0530. <https://doi.org/10.1371/journal.pcbi.0030055>.
- [37] C. He, Y. Wu, Y. Lai, Z. Cai, Y. Liu, L. Lai, Dynamic eicosanoid responses upon different inhibitor and combination treatments on the arachidonic acid metabolic network, *Molecular BioSystems*. 8 (2012) 1585–1594. <https://doi.org/10.1039/c2mb05503a>.
- [38] J. Dalli, Does promoting resolution instead of inhibiting inflammation represent the new paradigm in treating infections?, *Molecular Aspects of Medicine*. 58 (2017) 12–20. <https://doi.org/10.1016/j.mam.2017.03.007>.
- [39] V. Fattori, T.H. Zaninelli, F.S. Rasquel-Oliveira, R. Casagrande, W.A. Verri, Specialized pro-resolving lipid mediators: A new class of non-immunosuppressive and non-opioid analgesic drugs, *Pharmacological Research*. 151 (2020) 104549. <https://doi.org/10.1016/j.phrs.2019.104549>.

- [40] C. Kontogiorgis, M. Mantzanidou, D. Hadjipavlou-Litina, Chalcones and their potential role in inflammation., *Mini Reviews in Medicinal Chemistry*. 8 (2008) 1224–42. <https://doi.org/10.2174/138955708786141034>.
- [41] A.-M. Katsori, D. Hadjipavlou-Litina, Recent progress in therapeutic applications of chalcones., *Expert Opinion on Therapeutic Patents*. 21 (2011) 1575–96. <https://doi.org/10.1517/13543776.2011.596529>.
- [42] S. Sogawa, Y. Nihro, H. Ueda, A. Izumi, T. Miki, H. Matsumoto, T. Satoh, 3,4-Dihydroxychalcones as potent 5-lipoxygenase and cyclooxygenase inhibitors., *Journal of Medicinal Chemistry*. 36 (1993) 3904–9. <https://doi.org/10.1021/jm00076a019>.
- [43] Y. Koshihara, Y. Fujimoto, H. Inoue, A new 5-lipoxygenase selective inhibitor derived from *Artocarpus communis* strongly inhibits arachidonic acid-induced ear edema., *Biochemical Pharmacology*. 37 (1988) 2161–5. [https://doi.org/10.1016/0006-2952\(88\)90576-x](https://doi.org/10.1016/0006-2952(88)90576-x).
- [44] C. Nakamura, N. Kawasaki, H. Miyataka, E. Jayachandran, I.H. Kim, K.L. Kirk, T. Taguchi, Y. Takeuchi, H. Hori, T. Satoh, Synthesis and biological activities of fluorinated chalcone derivatives., *Bioorganic & Medicinal Chemistry*. 10 (2002) 699–706. [https://doi.org/10.1016/s0968-0896\(01\)00319-4](https://doi.org/10.1016/s0968-0896(01)00319-4).
- [45] M. Forino, S. Pace, G. Chianese, L. Santagostini, M. Werner, C. Weinigel, S. Rummeler, G. Fico, O. Werz, O. Taglialatela-Scafati, Humudifucol and Bioactive Prenylated Polyphenols from Hops (*Humulus lupulus* cv. “Cascade”)., *Journal of Natural Products*. 79 (2016) 590–7. <https://doi.org/10.1021/acs.jnatprod.5b01052>.
- [46] N.P. Reddy, P. Aparoy, T.C.M. Reddy, C. Achari, P.R. Sridhar, P. Reddanna, Design, synthesis, and biological evaluation of prenylated chalcones as 5-LOX inhibitors.,

Bioorganic & Medicinal Chemistry. 18 (2010) 5807–15.
<https://doi.org/10.1016/j.bmc.2010.06.107>.

- [47] M. Arockia Babu, N. Shakya, P. Prathipati, S.G. Kaskhedikar, A.K. Saxena, Development of 3D-QSAR models for 5-lipoxygenase antagonists: chalcones., *Bioorganic & Medicinal Chemistry*. 10 (2002) 4035–41. [https://doi.org/10.1016/s0968-0896\(02\)00313-9](https://doi.org/10.1016/s0968-0896(02)00313-9).
- [48] S. Sinha, S.L. Manju, M. Doble, Chalcone-Thiazole Hybrids: Rational Design, Synthesis, and Lead Identification against 5-Lipoxygenase., *ACS Medicinal Chemistry Letters*. 10 (2019) 1415–1422. <https://doi.org/10.1021/acsmchemlett.9b00193>.
- [49] A.N. Boshra, H.H.M. Abdu-Allah, A.F. Mohammed, A.M. Hayallah, Click chemistry synthesis, biological evaluation and docking study of some novel 2'-hydroxychalcone-triazole hybrids as potent anti-inflammatory agents., *Bioorganic Chemistry*. 95 (2020) 103505. <https://doi.org/10.1016/j.bioorg.2019.103505>.
- [50] P. Borgeat, Biochemistry of the lipoxygenase pathways in neutrophils., *Canadian Journal of Physiology and Pharmacology*. 67 (1989) 936–42. <https://doi.org/10.1139/y89-147>.
- [51] O. Werz, D. Steinhilber, Development of 5-lipoxygenase inhibitors - Lessons from cellular enzyme regulation, *Biochemical Pharmacology*. 70 (2005) 327–333. <https://doi.org/10.1016/j.bcp.2005.04.018>.
- [52] H. Sadeghian, A. Jabbari, 15-Lipoxygenase inhibitors: a patent review., *Expert Opinion on Therapeutic Patents*. 26 (2016) 65–88. <https://doi.org/10.1517/13543776.2016.1113259>.
- [53] O. Werz, Inhibition of 5-lipoxygenase product synthesis by natural compounds of plant origin, *Planta Medica*. 73 (2007) 1331–1357. <https://doi.org/10.1055/s-2007-990242>.

- [54] S.-Y. Cheung, M. Werner, L. Esposito, F. Troisi, V. Cantone, S. Liening, S. König, J. Gerstmeier, A. Koeberle, R. Bilancia, R. Rizza, A. Rossi, F. Roviezzo, V. Temml, D. Schuster, H. Stuppner, M. Schubert-Zsilavec, O. Werz, T. Hanke, S. Pace, Discovery of a benzenesulfonamide-based dual inhibitor of microsomal prostaglandin E2 synthase-1 and 5-lipoxygenase that favorably modulates lipid mediator biosynthesis in inflammation, *European Journal of Medicinal Chemistry*. 156 (2018) 815–830. <https://doi.org/10.1016/J.EJMECH.2018.07.031>.
- [55] J. Gerstmeier, J. Seegers, F. Witt, B. Waltenberger, V. Temml, J.M. Rollinger, H. Stuppner, A. Koeberle, D. Schuster, O. Werz, Ginkgolic Acid is a Multi-Target Inhibitor of Key Enzymes in Pro-Inflammatory Lipid Mediator Biosynthesis., *Frontiers in Pharmacology*. 10 (2019) 797. <https://doi.org/10.3389/fphar.2019.00797>.
- [56] T.T. Van Anh, A. Mostafa, Z. Rao, S. Pace, S. Schwaiger, C. Kretzer, V. Temml, C. Giesel, P.M. Jordan, R. Bilancia, C. Weinigel, S. Rummler, B. Waltenberger, T. Hung, A. Rossi, H. Stuppner, O. Werz, A. Koeberle, From Vietnamese plants to a biflavonoid that relieves inflammation by triggering the lipid mediator class switch to resolution, *Acta Pharmaceutica Sinica B*. 11 (2021) 1629–1647. <https://doi.org/10.1016/j.apsb.2021.04.011>.
- [57] R.G. Snodgrass, B. Brüne, Regulation and Functions of 15-Lipoxygenases in Human Macrophages, *Frontiers in Pharmacology*. 10 (2019) 1–12. <https://doi.org/10.3389/fphar.2019.00719>.